# PHOTOGRAMMETRY-DERIVED ORTHOIMAGERY AND ELEVATION DATA FOR KONGIGANAK, ALASKA, COLLECTED JUNE 7, 2023

Keith C. Horen, Nora M. Nieminski, Autumn C. Poisson, and Zachary J. Siemsen

Raw Data File 2024-20


Location maps showing the survey area.

This report has not been reviewed for technical content or for conformity to the editorial standards of DGGS.

2024
STATE OF ALASKA
DEPARTMENT OF NATURAL RESOURCES
DIVISION OF GEOLOGICAL & GEOPHYSICAL SURVEYS

**STATE OF ALASKA**
Mike Dunleavy, Governor

**DEPARTMENT OF NATURAL RESOURCES**
John Boyle, Commissioner

**DIVISION OF GEOLOGICAL & GEOPHYSICAL SURVEYS**
Melanie Werdon, State Geologist & Director

Publications produced by the Division of Geological & Geophysical Surveys are available to download from the DGGS website (dggs.alaska.gov). Publications on hard-copy or digital media can be examined or purchased in the Fairbanks office:

**Alaska Division of Geological & Geophysical Surveys (DGGS)**
3354 College Road | Fairbanks, Alaska 99709-3707
Phone: 907.451.5010 | Fax 907.451.5050
dggspubs@alaska.gov | dggs.alaska.gov

**DGGS publications are also available at:**

Alaska State Library, Historical
Collections & Talking Book Center
395 Whittier Street
Juneau, Alaska 99801

Alaska Resource Library and
Information Services (ARLIS)
3150 C Street, Suite 100
Anchorage, Alaska 99503

**Suggested citation:**

Horen, K.C., Nieminski, N.M., Poisson, A.C., and Siemsen, Z.J., 2024, Photogrammetry-derived orthoimagery and elevation data for Kongiganak, Alaska, collected June 7, 2023: Alaska Division of Geological & Geophysical Surveys Raw Data File 2024-20, 9 p. https://doi.org/10.14509/31288

# PHOTOGRAMMETRY-DERIVED ORTHOIMAGERY AND ELEVATION DATA FOR KONGIGANAK, ALASKA, COLLECTED JUNE 7, 2023

Keith C. Horen[1], Nora M. Nieminski[1], Autumn C. Poisson[1*], and Zachary J. Siemsen[1**]

## INTRODUCTION

The Alaska Division of Geological & Geophysical Surveys (DGGS) collected low-altitude aerial images from an unmanned aerial vehicle (UAV) in the community of Kongiganak, Alaska, on June 7, 2023. We used Structure-from-Motion (SfM) photogrammetry to produce two digital surface models (DSM) and two orthorectified images. The populated areas of Kongiganak were the focus of the primary aerial survey (fig. 1), while the secondary aerial survey covered the landfill to the northwest of the community (fig. 2). The orthoimage and elevation data are useful for assessing riverine hazards and changes over time. These products are released as a Raw Data File with an open end-user license. All files can be downloaded from https://doi.org/10.14509/31288 or elevation.alaska.gov.

## LIST OF DELIVERABLES

- Orthoimagery
- Digital Surface Model (DSM)
- Metadata

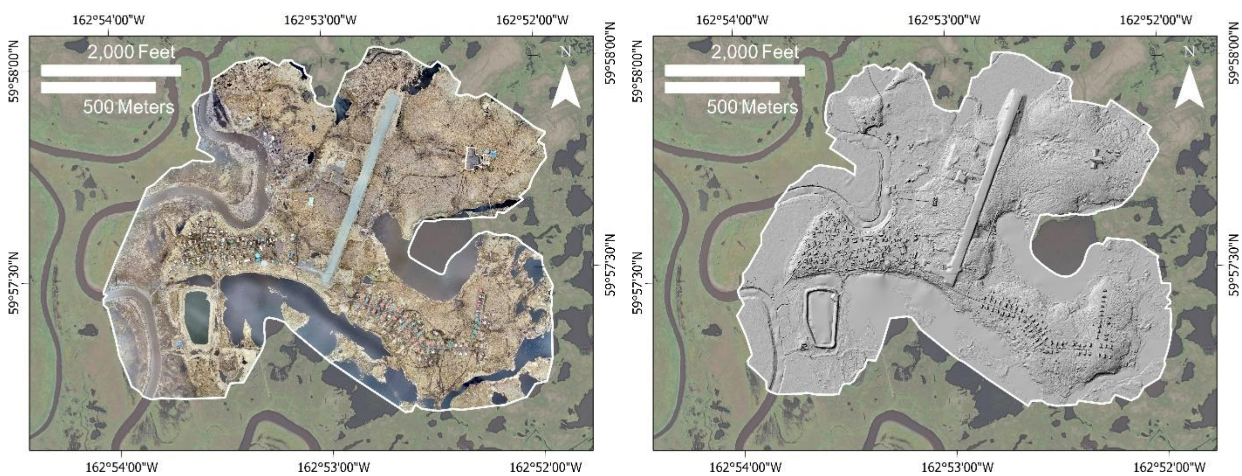


**Figure 1.** Extent of orthoimage (left) and digital surface model (DSM) (right) for the primary survey area.

[1] Alaska Division of Geological & Geophysical Surveys, 3354 College Road, Fairbanks, AK 99709

** Now at Dewberry, 8401 Arlington Blvd., Fairfax, Virginia 22031*

*** Now at PND Engineers, Inc., 1506 W 36th Ave., Anchorage, Alaska 99503*

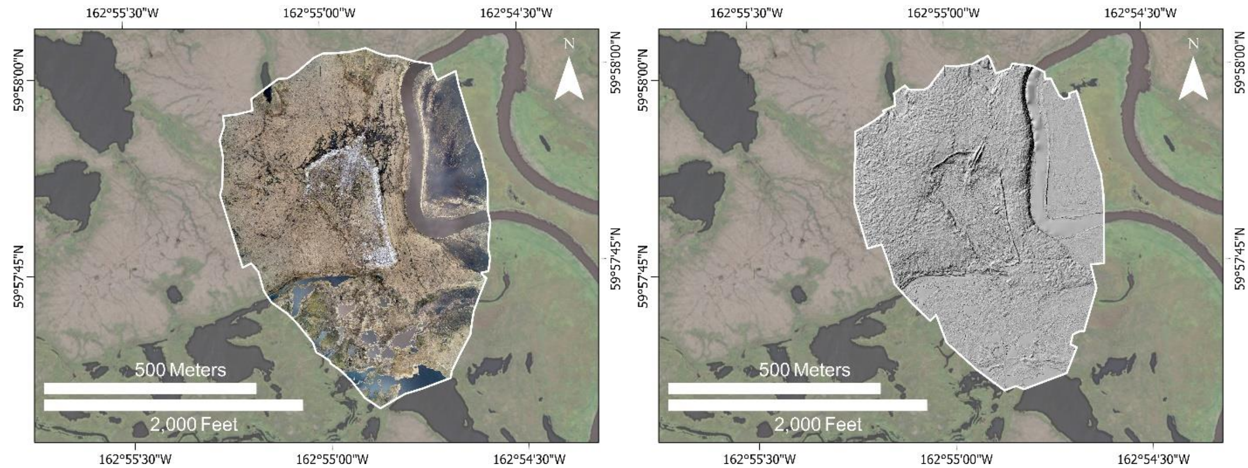


**Figure 2.** Extent of orthoimage (left) and digital surface model (DSM) (right) for the secondary survey area.

## METHODS

### Aerial Photogrammetric Survey Details

DGGS conducted flights on June 7, 2023, from approximately 4:15 PM to 8:30 PM AKDT using a DJI Phantom 4 RTK UAV with a FC6310R camera model (8.8 mm lens) to collect 1,813 20-megapixel JPEG photographs (5,472 x 3,648 pixels per image). The operator returned the UAV seven times to change batteries. DGGS flew the primary and secondary aerial surveys 120 m and 110 m above ground-level (AGL), respectively. Both surveys were flown with 75 percent side- and frontlap at 9.5 m/s, with nadir orientation stabilized using a three-axis gimbal. This resulted in images covering the primary survey area of 2.280 $km^2$ with a ground sampling distance (GSD) of 0.025 m and the secondary survey area of 0.395 $km^2$ with a ground sampling distance (GSD) of 0.022 m. The weather throughout the survey was mostly cloudy with light wind. No abnormalities were observed during the flights.

### Ground Survey Details

On June 7, 2023, DGGS temporarily installed a Trimble R10 receiver sampling at 5 Hz as a Global Navigation Satellite System (GNSS) base station over a temporary benchmark. This provided real-time kinematic (RTK) corrections to the ground rover, a Trimble R8s GNSS receiver. Using the ground rover, DGGS measured the location of 24 photo-identifiable ground control points (GCPs) within the primary survey area (fig. 3) and 10 within the secondary survey area (fig. 4).

### Data Processing

Base positions were corrected using Online Positioning User Service (OPUS) solutions (table 1), which were used to update the UAV and ground rover positions with post-processed kinematic (PPK) adjustments.

UAV positions were updated in RTKLIB (Version 2.4.3) software with the following settings applied: L1+L2 frequencies forward and backward filtered; a 10-degree elevation mask; receiver dynamics disabled; broadcast ionosphere and Saastamoinen troposphere corrections; a minimum fixed-ambiguity ratio of three; and L1/L2 code/carrier-phase error ratios of 100/100. During post-processing, DGGS applied International GNSS Service (IGS) precise orbits and final clock solutions retrieved from the Crustal Dynamics Data Information System (CDDIS) found at [urs.earthdata.nasa.gov](urs.earthdata.nasa.gov). Final corrected data were exported as time-stamped position files in WGS84 horizontal coordinate system with ellipsoidal heights and paired to corresponding photographs using an Aerotas P4RTK PPK Adjustments (Version 1) macro-enabled Microsoft Excel file.

Ground rover positions were updated using PPK corrections in Trimble Business Center (Version 5.51) software using default settings. Final corrected data were exported as comma-delimited text files in WGS84 horizontal coordinate system with ellipsoidal heights.

DGGS used Agisoft Metashape Professional (Version 1.8.3 build 14331) software for photogrammetric processing following the steps and settings outlined in Over and others (2021). During processing of the primary survey area, DGGS used 12 GCPs for photograph alignment and lens distortion parameter optimization (fig. 3, table 2), leaving 12 GCPs as horizontal and vertical check points (fig. 3, table 3). During processing of the secondary survey area, DGGS used 5 GCPs for photograph alignment and lens distortion parameter optimization (fig. 4, table 4), leaving 5 GCPs as horizontal and vertical check points (fig. 4, table 5). A confidence filter was applied to the resulting dense point cloud, eliminating all points derived from fewer than three discrete camera positions. Additional noise was removed from the dense point clouds through visual inspection.

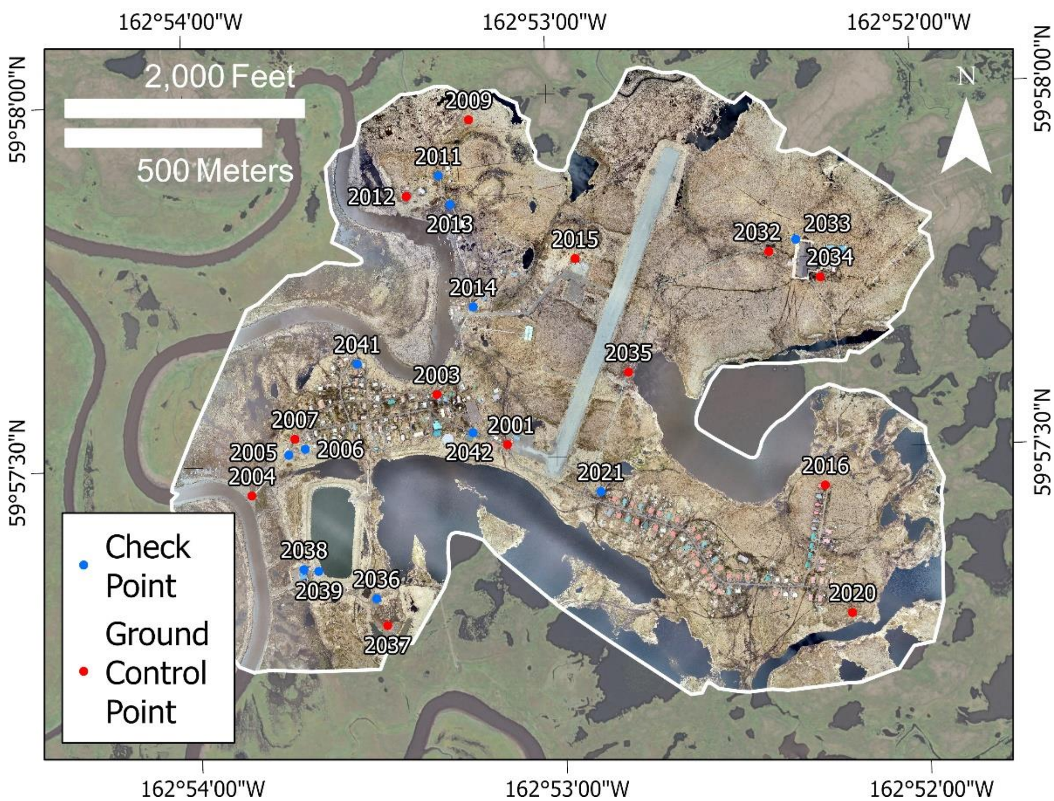


**Figure 3**. Location of photo-identifiable ground control points (GCP; red) and check points (CHK; blue) within the primary survey area.

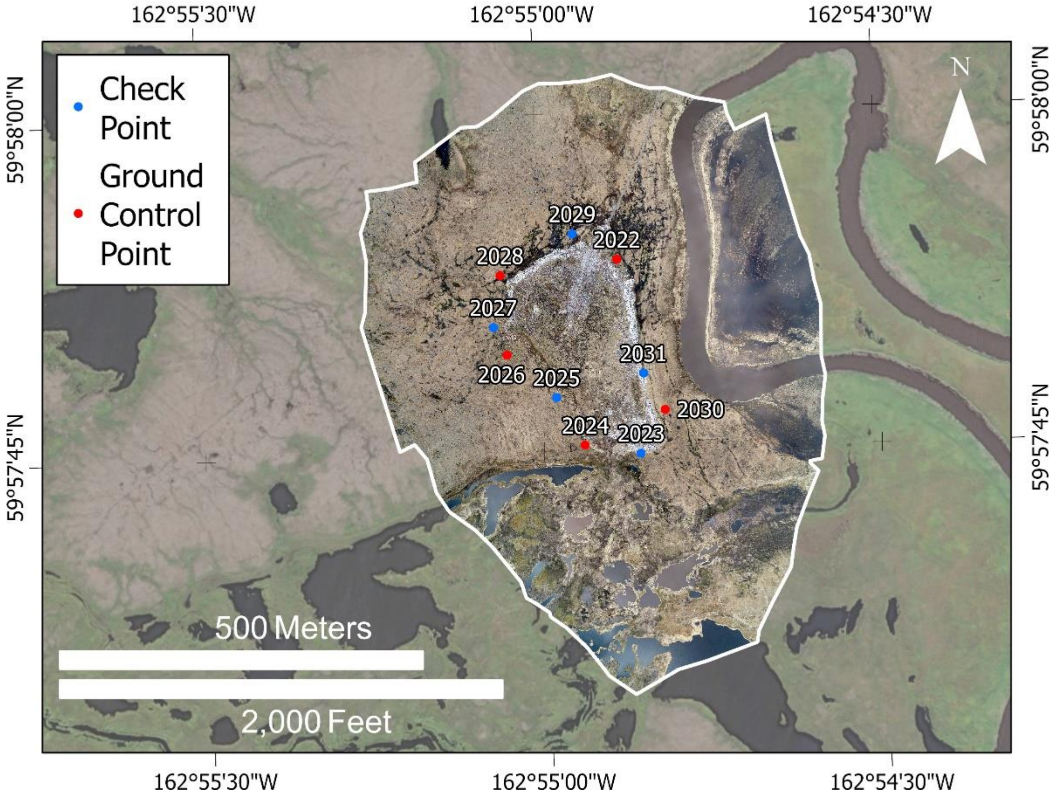


**Figure 4**. Location of photo-identifiable ground control points (GCP; red) and check points (CHK; blue) within the secondary survey area.

## IMAGERY PRODUCTS

### Orthoimagery

The orthoimages are three-band (red, green, blue), eight-bit unsigned GeoTIFF files with "No Data" values set to 0. The orthoimage of the primary survey area is derived from a color-adjusted mosaic of 1,362 aerial photographs with a GSD of 0.025 m per pixel. The orthoimage of the secondary survey area is derived from a color-adjusted mosaic of 230 aerial photographs with a GSD of 0.022 m per pixel.

### Digital Surface Model

The DSMs represent surface elevations including the height of vegetation, buildings, and other man-made features derived from the dense point clouds. The DSMs are single-band, 32-bit floating point GeoTIFF files with "No Data" values set to $-3.4028235 \times 10^{38}$. The DSM of the primary survey area was generated with a GSD of 0.049 m. The DSM of the secondary survey area was generated with a GSD of 0.045 m.

## ACCURACY REPORT

### Coordinate System and Datum

All data were processed in the WGS84 horizontal coordinate system and WGS84 ellipsoid vertical datum. All data were reprojected using Esri ArcGIS Pro (Version 3.0.2) software and are delivered in NAD83 (2011) UTM Zone 3N horizontal coordinate system and NAVD88 (GEOID12B) vertical datum.

### Horizontal Accuracy

DGGS quantified the horizontal accuracy of the GNSS position data using the latitudinal and longitudinal peak-to-peak errors provided by OPUS (table 1). Consistent with OPUS shared solution requirements (NOAA, 2022), DGGS considers high-quality GNSS solutions to have latitudinal and longitudinal errors less than or equal to 0.04 m.

We quantified the horizontal accuracy of the DSMs and orthoimages by comparing the known locations of photo-identifiable check points measured with GNSS against their modeled locations in the photogrammetric products (fig. 2). These are independent checkpoints not used during processing. X and Y errors are calculated as the root-mean-square (RMS) error of offsets. The primary survey area contained 12 check points, with X and Y errors of 0.043 m and 0.016 m, respectively, and a total horizontal error, the root-sum-square error of X and Y RMS errors, of 0.046 m (table 3). The secondary survey area contained 5 check points, with X and Y errors of 0.032 m and 0.013 m, respectively, and a total horizontal error of 0.035 m (table 5).

### Vertical Accuracy

DGGS quantified the vertical accuracy of the GNSS position data using the combined ellipsoidal height peak-to-peak errors provided by OPUS and orthometric height RMS error provided by NOAA's Vertical Datum Transformation software (NOAA, 2016; table 1). Consistent with OPUS shared solution requirements (NOAA, 2022), DGGS considers high-quality GNSS solutions to have vertical errors less than or equal to 0.08 m.

We quantified the vertical accuracy of the DSMs using the same check points used to quantify the horizontal accuracy. The RMS error of Z offsets is 0.023 m within the primary survey area (table 3) and 0.019 m within the secondary survey area (table 5). The total RMS error (X, Y, and Z) is 0.051 m within the primary survey area (table 3) and 0.040 m within the secondary survey area (table 5).

**Table 1.** Base station coordinates and GNSS errors.

| NAD83 (2011) Easting | NAD83 (2011) Northing | NAVD88 Elevation | GNSS X Error (m) | GNSS Y Error (m) | GNSS Z Error (m) |
|---|---|---|---|---|---|
| 618216.692 | 6648866.311 | 10.848 | 0.003 | 0.003 | 0.063 |

**Table 2.** Ground control point coordinates and offsets from primary survey area orthoimagery and DSM.

| Point | Easting | Northing | Elevation | X Offset (m) | Y Offset (m) | Z Offset (m) | GNSS X/Y Error (m) | GNSS Z Error (m) |
|---|---|---|---|---|---|---|---|---|
| 2001 | 618069.750 | 6648692.686 | 9.891 | -0.012 | 0.013 | -0.017 | 0.005 | 0.006 |
| 2003 | 617889.717 | 6648820.466 | 9.571 | 0.089 | 0.058 | -0.032 | 0.006 | 0.006 |
| 2004 | 617416.911 | 6648561.147 | 3.488 | -0.023 | -0.011 | -0.037 | 0.006 | 0.008 |
| 2007 | 617527.019 | 6648706.096 | 7.680 | -0.033 | 0.021 | -0.009 | 0.009 | 0.011 |
| 2009 | 617970.473 | 6649522.657 | 6.006 | 0.010 | 0.006 | 0.056 | 0.005 | 0.008 |
| 2012 | 617811.400 | 6649326.556 | 8.762 | -0.018 | -0.022 | 0.016 | 0.008 | 0.010 |
| 2015 | 618242.786 | 6649167.821 | 9.401 | -0.014 | -0.026 | 0.079 | 0.007 | 0.008 |
| 2016 | 618883.020 | 6648589.426 | 6.699 | -0.008 | 0.036 | -0.012 | 0.007 | 0.009 |
| 2020 | 618952.189 | 6648263.686 | 5.035 | -0.029 | -0.001 | 0.017 | 0.007 | 0.010 |
| 2032 | 618738.377 | 6649185.910 | 10.872 | 0.002 | 0.017 | -0.030 | 0.005 | 0.008 |
| 2034 | 618869.555 | 6649121.915 | 10.818 | 0.005 | -0.003 | -0.012 | 0.006 | 0.009 |
| 2035 | 618379.307 | 6648877.339 | 7.064 | 0.051 | 0.020 | -0.032 | 0.007 | 0.009 |
| | | | **Mean** | 0.002 | 0.009 | -0.001 | 0.006 | 0.008 |
| | | | **Standard Deviation** | 0.035 | 0.024 | 0.037 | 0.001 | 0.002 |
| | | | **Range** | 0.122 | 0.084 | 0.117 | 0.004 | 0.005 |
| | | | **Root Mean Square Error** | 0.034 | 0.023 | **0.035** | 0.001 | 0.001 |
| | | | **Total Error** | **0.041** | | **0.054** | **0.002** | |
| | | | | **(XY)** | | **(XYZ)** | **(XYZ)** | |

**Table 3.** Check point coordinates and offsets from primary survey area orthoimagery and DSM.

| Point | Easting | Northing | Elevation | X Offset (m) | Y Offset (m) | Z Offset (m) | GNSS X/Y Error (m) | GNSS Z Error (m) |
|---|---|---|---|---|---|---|---|---|
| 2005 | 617510.934 | 6648664.747 | 6.740 | 0.003 | 0.012 | -0.033 | 0.006 | 0.008 |
| 2006 | 617552.920 | 6648680.248 | 7.666 | 0.040 | 0.012 | 0.003 | 0.008 | 0.011 |
| 2011 | 617893.189 | 6649379.523 | 4.854 | 0.006 | 0.006 | 0.006 | 0.008 | 0.010 |
| 2013 | 617923.005 | 6649305.624 | 3.877 | -0.021 | -0.008 | -0.035 | 0.005 | 0.005 |
| 2014 | 617982.012 | 6649043.948 | 3.558 | 0.063 | -0.012 | -0.009 | 0.004 | 0.005 |
| 2021 | 618308.833 | 6648571.898 | 7.371 | 0.008 | 0.005 | 0.039 | 0.006 | 0.009 |
| 2033 | 618806.741 | 6649216.800 | 11.371 | -0.070 | -0.002 | -0.029 | 0.006 | 0.009 |

| Point | Easting | Northing | Elevation | X Offset (m) | Y Offset (m) | Z Offset (m) | GNSS X/Y Error (m) | GNSS Z Error (m) |
|---|---|---|---|---|---|---|---|---|
| 2036 | 617735.398 | 6648298.397 | 4.277 | 0.058 | 0.035 | 0.015 | 0.008 | 0.009 |
| 2038 | 617550.079 | 6648372.691 | 4.342 | 0.049 | -0.012 | -0.028 | 0.009 | 0.009 |
| 2039 | 617587.952 | 6648368.120 | 6.314 | 0.076 | -0.009 | 0.004 | 0.009 | 0.009 |
| 2041 | 617685.892 | 6648898.237 | 7.100 | 0.005 | 0.021 | 0.007 | 0.009 | 0.009 |
| 2042 | 617982.050 | 6648722.735 | 10.452 | 0.023 | 0.031 | 0.016 | 0.009 | 0.009 |
| **Mean** | | | | 0.020 | 0.007 | -0.004 | 0.007 | 0.009 |
| **Standard Deviation** | | | | 0.041 | 0.016 | 0.023 | 0.002 | 0.002 |
| **Range** | | | | 0.146 | 0.047 | 0.074 | 0.005 | 0.006 |
| **Root Mean Square Error** | | | | 0.043 | 0.016 | **0.023** | 0.002 | 0.002 |
| **Total Error** | | | | **0.046** | | **0.051** | **0.003** | |
| | | | | **(XY)** | | **(XYZ)** | **(XYZ)** | |

**Table 4.** Ground control point coordinates and offsets from secondary survey area orthoimagery and DSM.

| Point | Easting | Northing | Elevation | X Offset (m) | Y Offset (m) | Z Offset (m) | GNSS X/Y Error (m) | GNSS Z Error (m) |
|---|---|---|---|---|---|---|---|---|
| 2022 | 616421.861 | 6649331.288 | 8.004 | -0.028 | -0.020 | -0.036 | 0.008 | 0.009 |
| 2024 | 616378.744 | 6649075.408 | 4.736 | -0.016 | -0.005 | 0.010 | 0.018 | 0.017 |
| 2026 | 616271.243 | 6649199.301 | 7.283 | -0.016 | 0.001 | -0.002 | 0.012 | 0.015 |
| 2028 | 616261.155 | 6649308.616 | 7.493 | 0.000 | 0.002 | -0.008 | 0.011 | 0.014 |
| 2030 | 616488.823 | 6649124.750 | 5.167 | -0.005 | 0.003 | 0.015 | 0.007 | 0.009 |
| **Mean** | | | | -0.013 | -0.004 | -0.004 | 0.011 | 0.013 |
| **Standard Deviation** | | | | 0.011 | 0.010 | 0.020 | 0.005 | 0.004 |
| **Range** | | | | 0.028 | 0.023 | 0.051 | 0.012 | 0.008 |
| **Root Mean Square Error** | | | | 0.010 | 0.009 | **0.018** | 0.004 | 0.003 |
| **Total Error** | | | | **0.013** | | **0.022** | **0.005** | |
| | | | | **(XY)** | | **(XYZ)** | **(XYZ)** | |

**Table 5.** Check point coordinates and offsets from secondary survey area orthoimagery and DSM.

| Point | Easting | Northing | Elevation | X Offset (m) | Y Offset (m) | Z Offset (m) | GNSS X/Y Error (m) | GNSS Z Error (m) |
|---|---|---|---|---|---|---|---|---|
| 2023 | 616455.518 | 6649064.387 | 4.761 | 0.019 | -0.008 | 0.032 | 0.021 | 0.019 |
| 2025 | 616338.975 | 6649140.773 | 5.675 | 0.038 | -0.004 | -0.007 | 0.013 | 0.015 |
| 2027 | 616251.964 | 6649237.099 | 7.499 | -0.025 | 0.001 | -0.021 | 0.011 | 0.015 |
| 2029 | 616360.454 | 6649366.147 | 8.023 | 0.016 | 0.003 | 0.008 | 0.007 | 0.009 |
| 2031 | 616458.875 | 6649174.726 | 5.494 | 0.011 | 0.025 | 0.002 | 0.008 | 0.012 |
| | | | **Mean** | 0.012 | 0.003 | 0.003 | 0.012 | 0.014 |
| | | | **Standard Deviation** | 0.023 | 0.013 | 0.020 | 0.006 | 0.004 |
| | | | **Range** | 0.064 | 0.033 | 0.053 | 0.014 | 0.009 |
| | | | **Root Mean Square Error** | 0.032 | 0.013 | **0.019** | 0.005 | 0.003 |
| | | | **Total Error** | **0.035** | | **0.040** | **0.006** | |
| | | | | **(XY)** | | **(XYZ)** | **(XYZ)** | |

## Data Consistency and Completeness

DGGS visually inspected the orthoimage for data errors such as shifts, seamline mismatches, and water noise overlapping land. Visual errors common to these SfM photogrammetry products include discontinuous powerlines and distortion near high-angle features like buildings, as well as water boundaries. Highly reflective objects such as water bodies, metal roofs, and white paint may cause overexposure, leading to spurious elevation points. There were no significantly erroneous areas that required repair.

## ACKNOWLEDGMENTS

We thank the Native Village of Kongiganak for supporting the creation of these data products, made possible with National Fish and Wildlife Foundation's National Coastal Resilience Funding through our partners at the Alaska Native Tribal Health Consortium. The views and conclusions contained in this document are those of the authors and should not be interpreted as representing the opinions or policies of the Alaska Division of Geological & Geophysical Surveys, the U.S. Government, or the National Fish and Wildlife Foundation and its funding sources. Mention of trade names or commercial products does not constitute their endorsement by the Alaska Division of Geological & Geophysical Surveys, the U.S. Government, or the National Fish and Wildlife Foundation and its funding sources.

## REFERENCES

National Oceanic and Atmospheric Administration (NOAA), 2016, Estimation of vertical uncertainties in VDatum. https://vdatum.noaa.gov/docs/est_uncertainties.html

———2022, About OPUS: National Geodetic Survey webpage, retrieved from https://geodesy.noaa.gov/OPUS/about.jsp

Over, J.R., Ritchie, A.C., Kranenburg, C.J., Brown, J.A., Buscombe, D., Noble, T., Sherwood, C.R., Warrick, J.A., and Wernette, P.A., 2021, Processing coastal imagery with Agisoft Metashape Professional Edition, version 1.6—Structure from motion workflow documentation: U.S. Geological Survey Open-File Report 2021-1039, 46 p. https://doi.org/10.3133/ofr20211039